Differential Geometry Measures of Nonlinearity with Applications to Ground Target Tracking

Mahendra Mallick
Lockheed Martin ORINCON Corporation
4770 Eastgate Mall
San Diego, CA 92121-1970, USA
mahendra.mallick@lmco.com

Abstract - *Most ground target tracking problems involve nonlinear filtering due to nonlinearity in the measurement model. At present, a quantitative measure of nonlinearity and its relationship with the performance of the filtering algorithms are lacking. We quantify the degree of nonlinearity of a filtering problem using the differential geometry based measures of nonlinearity such as the parameter-effects curvature and intrinsic curvature. The algorithm for calculating these two measures of nonlinearity was first presented for a static least squares estimation problem. In this paper, we extend the approach to calculate these two measures of nonlinearity for a problem involving a linear system dynamic model and nonlinear measurement model using the maximum likelihood estimator. We present numerical results using simulated data for the constant velocity motion of a target with range and azimuth measurements.*

Keywords: Ground target tracking, nonlinear filtering, differential geometry measures of nonlinearity, parameter-effects curvature, intrinsic curvature.

1 Introduction

Sensors employed in ground target tracking systems include the ground moving target indication (GMTI) radar, synthetic aperture radar (SAR), unattended ground sensor (UGS), electro-optical (EO) sensor, and infrared (IR) sensor. The measurements for these sensors are nonlinear functions of the target state. Even if the target dynamic model is linear, the filtering problem is nonlinear due to nonlinearity in the measurement model. If the dynamic and measurement models are linear with additive Gaussian noises, then the Kalman filter (KF) [1, 2] is an optimal estimator in the minimum mean square error (MMSE) sense and provides closed form solutions. Closed-form expressions for the conditional mean and covariance in the KF completely characterize the posterior Gaussian distribution for the target state. In general, no optimal or closed form solution exists for the nonlinear filtering problem. The extended Kalman filter (EKF) [1, 2] is commonly used as an approximate filter when the target dynamic model or/and sensor measurement model is/are nonlinear. The EKF retains only the first order term in the Taylor series expansion of the nonlinear dynamic or/and measurement models. This linearization can often introduce large errors in the estimated state and filter calculated covariance when the degree of nonlinearity (DoN) and measurement errors are high.

Although the DoN is widely referred to in filtering problems, a systematic and quantitative characterization is lacking at present. In this paper, we characterize the DoN using curvature measures of nonlinearity (CMoN) from differential geometry. We use two relative curvature measures of nonlinearity [3-6], the *parameter-effects curvature* and *intrinsic curvature* to characterize the degree of nonlinearity of a filtering problem. The linearization used in the EKF represents a tangent plane approximation to the measurement function or the system dynamic function at the predicted state. The CMoN indicate whether the tangent plane approximation used in the EKF is a good approximation or not for a given problem. In this paper we analyze the DoN for the filtering problem where the dynamic model is linear and the measurement model is nonlinear. This is a common approach in most ground target tracking problems.

In this paper, we use the symbol ":=" to define a quantity and I_n to represent an $n \times n$ idenity matrix. The outline of the paper is as follows. Section 2 describes the statement of the problem. Section 3 derives expressions for the velocity and acceleration arrays [3, 4] needed to compute the two CMoN and Section 4 defines the two curvature measures of nonlinearity. Section 5 derives the curvature measures of nonlinearity using velocity and acceleration in an arbitrary direction [3, 4]. In Section 6, we present the dynamic model and nonlinear measurement model for the 2D range and azimuth measurements for calculating the parameter-effects curvature and intrinsic curvature. Finally, Sections 7 and 8 present numerical results and conclusions.

2 Statement of Problem

Let $x_k \in \Re^n$ and $z_k \in \Re^{m_k}$ denote target state and measurement at time t_k, respectively. The linear dynamic model and nonlinear measurement model commonly used in ground target tracking problems are described, respectively, by

$$x_k = \Phi_{k,k-1} x_{k-1} + w_{k,k-1}, \tag{2-1}$$

$$z_k = h_k(x_k) + n_k, \tag{2-2}$$

where $\Phi_{k,k-1} := \Phi(t_k, t_{k-1})$ is the state transition matrix and $w_{k,k-1} := w(t_k, t_{k-1})$ is the zero-mean white Gaussian integrated process noise. In (2-2), $h_k : \Re^n \to \Re^m$ and $n_k \sim N(0, R_k)$ represent the nonlinear measurement function and zero-mean white Gaussian measurement noise, respectively. Taylor series expansion of the

measurement function about the predicted state at time k, $\hat{x}_{k|k-1}$ gives

$$h_k(x_k) = h_k(\hat{x}_{k|k-1}) + H_k(\hat{x}_{k|k-1})(x_k - \hat{x}_{k|k-1}) + \text{higher order terms} \tag{2-3}$$

where

$$H_k(\hat{x}_{k|k-1}) = \left.\frac{\partial h_k(x_k)}{\partial x_k}\right|_{x_k=\hat{x}_{k|k-1}}. \tag{2-4}$$

The EKF [1, 2] uses the linear approximation

$$h_k(x_k) \approx h_k(\hat{x}_{k|k-1}) + H_k(\hat{x}_{k|k-1})(x_k - \hat{x}_{k|k-1}). \tag{2-5}$$

The linear approximation used in the EKF is a valid approximation if and only if the measurement function is relatively flat near $\hat{x}_{k|k-1}$ and hence the tangent plane approximation [3, 4] in (2-5) is a valid approximation. This requires the quantification of the degree of nonlinearity of the measurement function.

In order to analyze the degree of nonlinearity of a filtering problem it is sufficient to consider the dynamic model without the process noise

$$x_k = \Phi_{k,k-1} x_{k-1}, \tag{2-6}$$

and the nonlinear measurement model described by (2-2). We estimate the initial state of the system $\theta = x_1$ at time t_1 processing a collection of N measurements

$$z := (z_1, \quad z_2, \quad \ldots \quad z_N). \tag{2-7}$$

The measurement error covariance matrix is diagonal in most practical tracking problems where

$$R_k = diag(\sigma_{k,1}^2 \quad \ldots \quad \sigma_{k,m_k}^2). \tag{2-8}$$

We generate dimensionless measurements $\{y_k\}$ by the mapping

$$y_{k,i} := \frac{z_{k,i}}{\sigma_{k,i}}, \quad \eta_{k,i}(x_k) := \frac{h_{k,i}(x_k)}{\sigma_{k,m}}, \quad v_{k,i} := \frac{n_{k,i}}{\sigma_{k,i}}. \tag{2-9}$$

$$y_k = \eta_k(x_k) + v_k, \qquad v_k \sim N(0, I_{m_k}). \tag{2-10}$$

The resulting problem becomes a maximum likelihood (ML) estimation problem

$$\max_{\theta} \Lambda(\theta) = \max_{\theta} p(y \mid \theta). \tag{2-11}$$

where $\Lambda(\theta)$ is the likelihood of the parameter θ. Because of the structure of measurement model described by (2-2), we get

$$p(y \mid \theta) = p(y_1, \quad y_2, \quad \ldots \quad y_K \mid \theta) = \prod_{k=1}^{N} p(y_k \mid \theta). \tag{2-12}$$

Using (2-6), we have

$$x_k = \Phi_{k,1} x_1 = \Phi_{k,1}\theta. \tag{2-13}$$

Use of (2-13) in (2-10) gives

$$y_k = f_k(\theta) + v_k, \qquad k = 1, \ldots, N, \tag{2-14}$$

where

$$f_k(\theta) := \eta_k(\Phi_{k,1}\theta). \tag{2-15}$$

The measurement model in (2-14) gives

$$p(y_k \mid \theta) = N(y_k; f_k(\theta), I_{m_k}) = [(2\pi)^{m_k}]^{-1/2} e^{-\frac{1}{2}(y_k - f_k(\theta))'(y_k - f_k(\theta))}. \tag{2-16}$$

Maximization of the likelihood function $\Lambda(\theta)$ is equivalent to minimization of the cost function

$$J(\theta) := \frac{1}{2}\sum_{k=1}^{N}[y_k - f_k(\theta)]'[y_k - f_k(\theta)] = \frac{1}{2}\|y - f(\theta)\|^2 \tag{2-17}$$

where by re-indexing y and f according to M scalar components, we have

$$y := \begin{bmatrix} y_1 \\ \ldots \\ y_M \end{bmatrix}, \quad f(\theta) := \begin{bmatrix} f_1(\theta) \\ \ldots \\ f_M(\theta) \end{bmatrix}. \tag{2-18}$$

The linear approximation used in the ML estimation problem uses approximation for the the mapping $G: \Re^n \to \Re^M$,

$$f(\theta) = f(\hat{\theta}) + \dot{F}(\hat{\theta})(\theta - \hat{\theta}) + \frac{1}{2}(\theta - \hat{\theta})'\ddot{F}(\hat{\theta})(\theta - \hat{\theta}) + \text{higher order terms}, \tag{2-19}$$

where

$$\dot{F}(\hat{\theta}) = \left.\frac{\partial f(\theta)}{\partial \theta}\right|_{\theta=\hat{\theta}}, \quad \dot{F}(\hat{\theta}) \in \Re^{M\times n}, \tag{2-20}$$

$$\ddot{f}_{mij}(\hat{\theta}) = \left.\frac{\partial^2 f_m(\theta)}{\partial\theta_i \partial\theta_j}\right|_{\theta=\hat{\theta}}, \quad \ddot{F}(\hat{\theta}) \in \Re^{M\times n\times n}, m = 1, \ldots, M,\ i, j = 1, \ldots, n. \tag{2-21}$$

Using the linear approximation in (2-19), we get

$$f(\theta) \approx f(\hat{\theta}) + \dot{F}(\hat{\theta})(\theta - \hat{\theta}). \tag{2-22}$$

According to the linear approximation, $f(\theta)$ lies in the plane tangent to the measurement surface at the point $\hat{\theta}$. Therefore, the linearization is equivalent to approximating the measurement surface by the tangent plane at $\hat{\theta}$ [3, 4]. The tangent plane is a good approximation to the measurement surface if the magnitude of the quadratic term, $\left\|(\theta - \hat{\theta})'\ddot{F}(\hat{\theta})(\theta - \hat{\theta})\right\|$ is negligible compared with the magnitude of the linear term $\left\|\dot{F}(\hat{\theta})(\theta - \hat{\theta})\right\|$. Each term in (3-15) is an $M \times 1$ vector. It is useful to decompose the quadratic term on the right hand side of (2-19) into

components in the tangent plane and orthogonal to the tangent plane.

3 Velocity and Acceleration Vectors

Define the $(M \times 1)$ *velocity vectors* or *tangent vectors* [3, 4]

$$\dot{f}_i(\hat{\theta}) := \left.\frac{\partial f(\theta)}{\partial \theta_i}\right|_{\theta=\hat{\theta}} = \left[\left.\frac{\partial f_1(\theta)}{\partial \theta_i}\right|_{\theta=\hat{\theta}} \quad ... \quad \left.\frac{\partial f_M(\theta)}{\partial \theta_i}\right|_{\theta=\hat{\theta}}\right]' \quad i = 1,2,...,n. \tag{3-1}$$

Then

$$\dot{F}(\hat{\theta}) = [\dot{f}_1(\hat{\theta}) \quad ... \quad \dot{f}_n(\hat{\theta})]. \tag{3-2}$$

The velocity vectors span an *n*-dimensional space, the *tangent plane*. We define the $(M \times 1)$ *acceleration vectors* [3, 4]

$$\ddot{f}_{ij}(\hat{\theta}) := \left.\frac{\partial^2 f(\theta)}{\partial \theta_i \partial \theta_j}\right|_{\theta=\hat{\theta}}, \quad i, j = 1,...,n. \tag{3-3}$$

The acceleration vectors have the following properties:

$$\ddot{f}_{ij}(\hat{\theta}) = \ddot{f}_{ji}(\hat{\theta}), \quad i, j = 1,2,...,n \tag{3-4}$$

$$\ddot{f}_{ij}(\hat{\theta}) = \left.\frac{\partial \dot{f}_i(\theta)}{\partial \theta_j}\right|_{\theta=\hat{\theta}} = \left.\frac{\partial \dot{f}_j(\theta)}{\partial \theta_i}\right|_{\theta=\hat{\theta}}, \quad i, j = 1,2,...,n. \tag{3-5}$$

Because of the property (3-4), there are n_a distinct acceleration vectors, where $n_a = n \times (n+1)/2$. We want to decompose the acceleration vectors into components in the tangent plane and orthogonal to the tangent plane.

Let $\ddot{F}_m(\hat{\theta}) \in \Re^{n \times n}$ denote the the m^{th} face [3, 4] of the accelaration array $\ddot{F}(\hat{\theta})$, where $\ddot{F}_m(\hat{\theta})$ is defined by

$$\ddot{F}_m(\hat{\theta}) := \begin{bmatrix} \ddot{f}_{m11}(\hat{\theta}) & ... & \ddot{f}_{m1n}(\hat{\theta}) \\ ... & ... & ... \\ \ddot{f}_{mn1}(\hat{\theta}) & ... & \ddot{f}_{mnn}(\hat{\theta}) \end{bmatrix}, \quad m = 1,2,...,M. \tag{3-6}$$

The projection matrix P_T which projects an *n*-vector into the tangent plane is defined by [4]

$$P_T := \dot{F}(\hat{\theta})(\dot{F}'(\hat{\theta})\dot{F}(\hat{\theta}))^{-1}\dot{F}'(\hat{\theta}). \tag{3-7}$$

Therefore, we can decompose an acceleration vector into components tangent and orthogonal to the tangent plane. Let $\ddot{f}_{ij}^T(\hat{\theta})$ and $\ddot{f}_{ij}^N(\hat{\theta})$ denote the tangential and orthogonal components of the acceleration vector $\ddot{f}_{ij}(\hat{\theta})$, respectively. Then

$$\ddot{f}_{ij}^T(\hat{\theta}) = P_T \ddot{f}_{ij}(\hat{\theta}), \quad i, j = 1,2,...,n, \tag{3-8}$$

$$\ddot{f}_{ij}^N(\hat{\theta}) = (I - P_T)\ddot{f}_{ij}(\hat{\theta}), \quad i, j = 1,2,...,n. \tag{3-9}$$

$$\ddot{f}_{ij}(\hat{\theta}) = \ddot{f}_{ij}^T(\hat{\theta}) + \ddot{f}_{ij}^N(\hat{\theta}), \quad \text{with } \ddot{f}_{ij}^T \perp \ddot{f}_{ij}^N, \quad i, j = 1,2,...,n. \tag{3-10}$$

Use of (3-10) for the quadratic term in in (2-19) gives

$$\left\|\delta'\ddot{F}(\hat{\theta})\delta\right\|^2 = \left\|\delta'\ddot{F}^T(\hat{\theta})\delta\right\|^2 + \left\|\delta'\ddot{F}^N(\hat{\theta})\delta\right\|^2, \tag{3-11}$$

where

$$\delta := (\theta - \hat{\theta}). \tag{3-12}$$

4 Curvature Measures of Nonlinearity

Bates and Watts define *parameter-effects curvature* K_δ^T and *intrinsic curvature* K_δ^N [3-6] as two measures of nonlinearity which compares the quadratic term with the linear term in the direction of the vector δ in the parameter space. These two curvatures at $\hat{\theta}$ along δ are defined by [3-6]

$$K_\delta^T := \frac{\left\|\delta'\ddot{F}^T(\hat{\theta})\delta\right\|}{\left\|\dot{F}(\hat{\theta})\delta\right\|^2} \tag{4-1}$$

$$K_\delta^N := \frac{\left\|\delta'\ddot{F}^N(\hat{\theta})\delta\right\|}{\left\|\dot{F}(\hat{\theta})\delta\right\|^2}. \tag{4-2}$$

Let $u \in \Re^n$ be a unit vector along δ and b be the norm of δ. Then

$$\delta := \|\delta\|u = bu. \tag{4-3}$$

Use of (4-3) in (4-1) and (4-2) gives

$$K_u^T := \frac{\left\|u'\ddot{F}^T(\hat{\theta})u\right\|}{\left\|\dot{F}(\hat{\theta})u\right\|^2}, \tag{4-4}$$

$$K_u^N := \frac{\left\|u'\ddot{F}^N(\hat{\theta})u\right\|}{\left\|\dot{F}(\hat{\theta})u\right\|^2}. \tag{4-5}$$

The curvature K_u^T along the direction u at $\hat{\theta}$ depends on the type of parametrization used. Therefore, it is known as the parameter-effects curvature. On the other hand, the curvature K_u^N in direction u at $\hat{\theta}$ is an intrinsic property of the measurement surface and does not depend on the type of parametrization used.

Bates and Watts [3, 4] defined scale-free curvatures by multiplying the curvatures K_u^T and K_u^N by the *standard radius* ρ [3, 4] to obtain

$$\gamma_u^T := \rho K_u^T, \tag{4-6}$$

$$\gamma_u^N := \rho K_u^N, \tag{4-7}$$

$$\rho := s\sqrt{n} = \left\|y - f(\hat{\theta})\right\|\sqrt{\frac{n}{M-n}}. \tag{4-8}$$

5 Curvatures using Velocity and Acceleration in an Arbitrary Direction

To calculate the relative curvatures, we need to calculate the acceleration vetors in an arbitrary direction [3, 4]. Let $u \in \Re^n$ be an arbitrary unit vector in the parameters space. To calculate the velocity and acceleration vectors near $\hat{\theta}$ in an arbitrary direction *u*, we treat θ as a function of a distance parameter *b* and define

$$\theta(b,u) := \hat{\theta} + bu. \tag{5-1}$$

Equation (5-1) represents a straight line in the parameters space passing through $\hat{\theta}$. Mapping of the line in the parameters space to the measurement space using (5-1) in $f(\theta)$, generates the parametric curve

$$f_u(b) := f(\theta(b,u)) = f(\hat{\theta} + bu) \tag{5-2}$$

passing through the point $f(\hat{\theta})$. Define

$$\dot{f}_u(b) := \frac{\partial f_u(b)}{\partial b}. \tag{5-3}$$

Then

$$\dot{f}_u(b) = \sum_{i=1}^{n} \frac{\partial f(\theta)}{\partial \theta_i} \frac{\partial \theta_i(b,u)}{\partial b} = \sum_{i=1}^{n} \dot{f}_i(\theta) u_i. \tag{5-4}$$

We can write (5-4) compactly by

$$\dot{f}_u(b) = \dot{F}(\theta) u. \tag{5-5}$$

Similarly, define

$$\ddot{f}_u(b) := \frac{\partial^2 f_u(b)}{\partial b^2}. \tag{5-6}$$

Differentiating $\dot{f}_u(b)$ with respect to *b*, we get

$$\begin{aligned} \ddot{f}_u(b) &= \frac{\partial}{\partial b} \sum_{i=1}^{n} \dot{f}_i(\theta) u_i \\ &= \sum_{i=1}^{n} \sum_{j=1}^{n} \frac{\partial}{\partial \theta_j} \left[\dot{f}_i(\theta) u_i \right] \frac{\partial \theta_j}{\partial b} \\ &= \sum_{i=1}^{n} \sum_{j=1}^{n} \left[\frac{\partial \dot{f}_i(\theta)}{\partial \theta_j} u_i + \dot{f}_i(\theta) \frac{\partial u_i}{\partial b} \right] u_j \\ &= \sum_{i=1}^{n} \sum_{j=1}^{n} \ddot{f}_{ij}(\theta) u_i u_j, \end{aligned} \tag{5-7}$$

since $\partial u_i / \partial b = 0$. We can compactly write (5-7) by

$$\ddot{f}_u(b) = u' \ddot{F}(\theta) u. \tag{5-8}$$

Setting *b* equal to zero in (5-5) and (5-8) we get, respectively,

$$\dot{f}_u(0) = \dot{F}(\hat{\theta}) u, \tag{5-9}$$

$$\ddot{f}_u(0) = u' \ddot{F}(\hat{\theta}) u. \tag{5-10}$$

By orthogonal decomposition of $\ddot{f}_u(0)$, we have

$$\ddot{f}_u(0) = \ddot{f}_u^T(0) + \ddot{f}_u^N(0). \tag{5-11}$$

Then the curvatures at $\hat{\theta}$ in the direction u are

$$K_u^T := \frac{\left\| u' \ddot{F}^T(\hat{\theta}) u \right\|}{\left\| \dot{F}(\hat{\theta}) u \right\|^2} = \frac{\left\| \ddot{f}_u^T(0) \right\|}{\left\| \dot{f}_u(0) \right\|^2}, \tag{5-12}$$

$$K_u^N := \frac{\left\| u' \ddot{F}^N(\hat{\theta}) u \right\|}{\left\| \dot{F}(\hat{\theta}) u \right\|^2} = \frac{\left\| \ddot{f}_u^N(0) \right\|}{\left\| \dot{f}_u(0) \right\|^2}. \tag{5-13}$$

Consider the *QR* factorization [7, 8] of $\dot{F}(\hat{\theta})$:

$$\dot{F}(\hat{\theta}) = QR = [Q_n \quad Q_{M-n}] \begin{bmatrix} R_{11} \\ 0_{(M-n)\times n} \end{bmatrix} = Q_n R_{11}, \tag{5-14}$$

where Q_n is the first *n* columns of *Q*, Q_{M-n} is the next $(M-n)$ columns of *Q*, and R_{11} is an $n \times n$ nonsingular upper triangular matrix. Then use of (5-14) in (5-9) gives

$$\dot{f}_u(0) = \dot{F}(\hat{\theta}) u = Q_n R_{11} u = Q_n d, \tag{5-15}$$

where

$$d := R_{11} u. \tag{5-16}$$

Consider the mapping

$$\phi = R_{11} \theta. \tag{5-17}$$

Then

$$\theta = K\phi, \tag{5-18}$$

where

$$K = R_{11}^{-1}. \tag{5-19}$$

Substituting the expression for θ from (5-18) in $f(\theta)$, we get

$$f(\theta) = f(K\phi) = g(\phi). \tag{5-20}$$

Define

$$\dot{g}_i(\phi) := \frac{\partial g(\phi)}{\partial \phi_i}, \tag{5-21}$$

$$\ddot{g}_{ij}(\phi) := \frac{\partial^2 g(\phi)}{\partial \phi_i \phi_j} = \frac{\partial \dot{g}_i(\phi)}{\partial \phi_j} = \frac{\partial \dot{g}_j(\phi)}{\partial \phi_i}. \tag{5-22}$$

Then

$$\dot{f}_u(b) = \sum_{i=1}^{n} \dot{g}_i(\phi) d_i = \dot{G}(\phi) d, \tag{5-23}$$

$$\dot{G}(\phi) = [\dot{g}_1(\phi) \quad \ldots \quad \dot{g}_n(\phi)], \tag{5-24}$$

$$\dot{f}_u(0) = \dot{G}(\hat{\phi}) d = \dot{F}(\hat{\theta}) u. \tag{5-25}$$

Use of (5-16) in (5-25) gives

$$\begin{aligned} \dot{G}(\hat{\phi}) d = \dot{G}(\hat{\phi}) R_{11} u = \dot{F}(\hat{\theta}) u, \\ \text{or} \qquad \dot{G}(\hat{\phi}) = \dot{F}(\hat{\theta}) R_{11}^{-1}. \end{aligned} \tag{5-26}$$

Using the *QR* factorization of $\dot{F}(\hat{\theta})$ from (5-14) in (5-26) gives

$$\dot{G}(\hat{\phi}) = \dot{F}(\hat{\theta})R_{11}^{-1} = Q_n R_{11} R_{11}^{-1} = Q_n. \tag{5-27}$$

From (5-21) we get

$$\begin{aligned} \dot{g}_i(\phi) &= \frac{\partial g(\phi)}{\partial \phi_i} = \frac{\partial f(\theta)}{\partial \phi_i} \\ &= \sum_{j=1}^{n} \frac{\partial f(\theta)}{\partial \theta_j} \frac{\partial \theta_j}{\partial \phi_i} = \sum_{j=1}^{n} \dot{f}_j(\theta) \frac{\partial \theta_j}{\partial \phi_i}. \end{aligned} \tag{5-28}$$

From (5-18), we have

$$\theta_j = \sum_{l=1}^{n} k_{jl} \phi_l. \tag{5-29}$$

Thus

$$\frac{\partial \theta_j}{\partial \phi_i} = \sum_{l=1}^{n} k_{jl} \frac{\partial \phi_l}{\partial \phi_i} = \sum_{l=1}^{n} k_{jl} \delta_{il} = k_{ji}. \tag{5-30}$$

Substitution of (5-30) in (5-28) gives

$$\dot{g}_i(\phi) = \sum_{j=1}^{n} \dot{f}_j(\theta) k_{ji} = \dot{F}(\theta) k_i. \tag{5-31}$$

Differentiation of $\dot{g}_i(\phi)$ in (5-31) with respect to ϕ_j gives

$$\begin{aligned} \ddot{g}_{ij}(\phi) &= \frac{\partial \dot{g}_i(\phi)}{\partial \phi_j} = \frac{\partial}{\partial \phi_j} \sum_{p=1}^{n} \dot{f}_p(\theta) k_{pi} \\ &= \sum_{p=1}^{n} \frac{\partial \dot{f}_p(\theta)}{\partial \phi_j} k_{pi} = \sum_{p=1}^{n} \sum_{q=1}^{n} \frac{\partial \dot{f}_p(\theta)}{\partial \theta_q} \frac{\partial \theta_q}{\partial \phi_j} k_{pi}, \\ &= \sum_{p=1}^{n} \sum_{q=1}^{n} \ddot{f}_{pq}(\theta) k_{pi} k_{qj} = \sum_{p=1}^{n} \sum_{q=1}^{n} k'_{ip} \ddot{f}_{pq}(\theta) k_{qj}. \end{aligned} \tag{5-32}$$

We can write (5-32) in a compact form by

$$\ddot{G}(\phi) = K' \ddot{F}(\theta) K, \tag{5-33}$$

$$\ddot{G}_m(\phi) = K' \ddot{F}_m K, \quad m = 1,2,...,M. \tag{5-34}$$

Using the derivative arrays $\dot{G}(\hat{\phi})$, $\ddot{G}^T(\hat{\phi})$, and $\ddot{G}^N(\hat{\phi})$ we can express the curvatures by

$$\gamma_u^T = \rho \frac{\left\| \ddot{f}_u^T(0) \right\|}{\left\| \dot{f}_u(0) \right\|^2} = \rho \frac{\left\| d' \ddot{G}^T(\hat{\phi}) d \right\|}{\left\| \dot{G}(\hat{\phi}) d \right\|^2}, \tag{5-35}$$

$$\gamma_u^N = \rho \frac{\left\| \ddot{f}_u^N(0) \right\|}{\left\| \dot{f}_u(0) \right\|^2} = \rho \frac{\left\| d' \ddot{G}^N(\hat{\phi}) d \right\|}{\left\| \dot{G}(\hat{\phi}) d \right\|^2}. \tag{5-36}$$

The denominator in (5-35) and (5-36) is simplified by

$$\begin{aligned} \left\| \dot{G}(\hat{\phi}) d \right\|^2 &= (\dot{G}(\hat{\phi}) d)' \dot{G}(\hat{\phi}) d \\ &= (Q_n d)' Q_n d = d' Q_n' Q_n d \\ &= d' I_n d = d' d = \|d\|^2. \end{aligned} \tag{5-37}$$

Let $u_d \in \Re^n$ be a unit vector along *d*. Then

$$d = \|d\| u_d, \quad \|u_d\| = 1. \tag{5-38}$$

Substitution of (5-38) in (5-35) and (5-36) gives

$$\gamma_u^T = \rho \frac{\left\| d' \ddot{G}^T(\hat{\phi}) d \right\|}{\|d\|^2} = \rho \left\| u_d' \ddot{G}^T(\hat{\phi}) u_d \right\|, \tag{5-39}$$

$$\gamma_u^N = \rho \frac{\left\| d' \ddot{G}^N(\hat{\phi}) d \right\|}{\|d\|^2} = \rho \left\| u_d' \ddot{G}^N(\hat{\phi}) u_d \right\|. \tag{5-40}$$

Suppose we apply the transformation Q' to an *M*-vector $x \in \Re^M$. Then

$$\|Q'x\|^2 = x'QQ'x = x' I_M x = x'x = \|x\|^2. \tag{5-41}$$

Applying the transformation Q' to $\ddot{f}_u(0)$, we get

$$Q' \ddot{f}_u(0) = \begin{bmatrix} \xi_1 \\ \xi_2 \end{bmatrix}, \tag{5-42}$$

where

$$Q_n' \ddot{f}_u^T(0) = \begin{bmatrix} \xi_1 \\ 0_{(M-n)\times 1} \end{bmatrix}, \tag{5-43}$$

$$Q_n' \ddot{f}_u^N(0) = \begin{bmatrix} 0_{n\times 1} \\ \xi_2 \end{bmatrix}. \tag{5-44}$$

Then

$$\begin{aligned} \left\| \ddot{f}_u^T(0) \right\| &= \left\| Q' \ddot{f}_u^T(0) \right\| = \left\| \begin{bmatrix} \xi_1 \\ 0 \end{bmatrix} \right\| = \|\xi_1\| \\ &= \left\| \sum_{i=1}^{n} \sum_{j=1}^{n} Q_n' \ddot{g}_{ij} d_i d_j \right\| = \left\| \sum_{i=1}^{n} \sum_{j=1}^{n} \ddot{a}_{ij}^T d_i d_j \right\| \\ &= \left\| d' \ddot{A}^T d \right\| = \left[\sum_{m=1}^{n} \left| d' \ddot{A}_m d \right|^2 \right]^{1/2}, \end{aligned} \tag{5-45}$$

where

$$a_{ij:} := Q' \ddot{g}_{ij}(\hat{\phi}). \tag{5-46}$$

We define the following transformed acceleraion array

$$\ddot{A} := [Q'][\ddot{G}(\hat{\phi})] = [Q' \ddot{g}_{ij}] = [\ddot{a}_{ij}]. \tag{5-47}$$

Thus using the transformed acceleration array, the curvatures are given by

$$\gamma_d^T = \rho \left[\sum_{m=1}^{n} \left| u_d' \ddot{A}_m u_d \right|^2 \right]^{1/2}, \tag{5-48}$$

$$\gamma_d^N = \rho \left[\sum_{m=n+1}^{M} \left| u_d' \ddot{A}_m u_d \right|^2 \right]^{1/2}. \tag{5-49}$$

6 Constant Velocity Motion with Range Azimuth Measurements

We consider the ML estimation problem for a target with a constant velocity motion (CVM) in the XY-plane with 2D range and azimuth measurements. An unattended ground sensor (UGS) with an acoustic and seismic sensor package or a radar sensor collects such measurements. Let $(p_x(t), p_y(t))$ and $(s_x(t), s_y(t))$ be the target and sensor positions at time *t*, respectively. Let $(r_x(t), r_y(t))$ denote the components of the 2D range vector. Then

$$\begin{bmatrix} r_x(t) \\ r_y(t) \end{bmatrix} = \begin{bmatrix} p_x(t) - s_x(t) \\ p_y(t) - s_y(t) \end{bmatrix}. \tag{6-1}$$

Omitting the measurement subscript k in (2-2), the measurement models for range and azimuth are

$$h_r(x,s) = r = [(p_x - s_x)^2 + (p_y - s_y)^2]^{1/2}, \tag{6-2}$$

$$h_\alpha(x,s) = \alpha = \begin{cases} \tan^{-1}(p_x - s_x, p_y - s_y), & \text{if } \tan^{-1}(r_x, r_y) > 0, \\ \tan^{-1}(p_x - s_x, p_y - s_y) + 2\pi, & \text{if } \tan^{-1}(r_x, r_y) < 0. \end{cases} \tag{6-3}$$

The derivative of the measurement function *h* with respect to the target state *x* is

$$H(x,s) := \frac{\partial h(x,s)}{\partial x} = \begin{bmatrix} u_x & u_y & 0 & 0 \\ r_y / r^2 & -r_x / r^2 & 0 & 0 \end{bmatrix}, \tag{6-4}$$

where *u* is a unit vector along the range vector defined by

$$u := \begin{bmatrix} u_x \\ u_y \end{bmatrix} = \frac{1}{r} \begin{bmatrix} p_x - s_x \\ p_y - s_y \end{bmatrix}. \tag{6-5}$$

In order to evaluate $\dot{F}(\theta)$, we need $\partial h(x_k, s_k)/\partial\theta$ which is calculated by

$$\frac{\partial h(x_k,s_k)}{\partial \theta} = \frac{\partial h(x_k,s_k)}{\partial x_k} \frac{\partial x_k}{\partial \theta} = \frac{\partial h(x_k,s_k)}{\partial x_k} \Phi_{k,1}. \tag{6-6}$$

For the current problem, the m^{th} face of the accelaration array $\ddot{F}_m(\hat{\theta})$ involves two types of terms corresponding to range and azimuth measurement functions. Thus, we need evaluation of two types of $n \times n$ Hessian matrices, $\partial^2 r / \partial\theta^2$ and $\partial^2 \alpha / \partial\theta^2$. It can be shown that

$$\frac{\partial^2 r_k}{\partial \theta^2} = \Phi'_{k,1} \frac{\partial H'_{r_k}}{\partial x_k} \Phi_{k,1}, \tag{6-8}$$

$$\frac{\partial^2 \alpha_k}{\partial \theta^2} = \Phi'_{k,1} \frac{\partial H'_{\alpha_k}}{\partial x_k} \Phi_{k,1}, \tag{6-9}$$

where

$$\frac{\partial H'_{r_k}}{\partial x_k} = \begin{bmatrix} \dfrac{\partial u_k}{\partial p_k} & 0_{2\times 2} \\ 0_{2\times 2} & 0_{2\times 2} \end{bmatrix}, \tag{6-10}$$

$$\frac{\partial u}{\partial p} = \frac{1}{r}[I_2 - uu'], \tag{6-11}$$

$$\frac{\partial H'_{\alpha_k}}{\partial x_k} = \begin{bmatrix} \Psi_k & 0_{2\times 2} \\ 0_{2\times 2} & 0_{2\times 2} \end{bmatrix}, \tag{6-12}$$

$$\Psi := \frac{1}{r^2} \begin{bmatrix} -2u_x u_y & 2u_x^2 - 1 \\ 2u_x^2 - 1 & 2u_x u_y \end{bmatrix}. \tag{6-13}$$

7 Numerical Simulation and Results

We assume that the sensor is located at the origin of the XY coordinate frame. The speed of the target is 10 km/hr and the velocity makes an angle of 45 degrees with the X-axis, as shown in Fig. 1. We vary the distance of closest approach (*D*) of the target from the sensor to analyze the curvature measures of nonlinearity. We consider three values, 1 km, 4 km, and 10 km for the distance of closest approach. We simulate the 2D range and azimuth measurements using a measurement error standard deviation of 20 meters for range and measurement error standard deviations of 3 degrees and 10 degrees for azimuth. For each scenario, we simulate 50 range and azimuth measurements. Figure 1 presents the truth trajectory of the target, senor location, and measurement locations with 0.99 probability error ellipses.

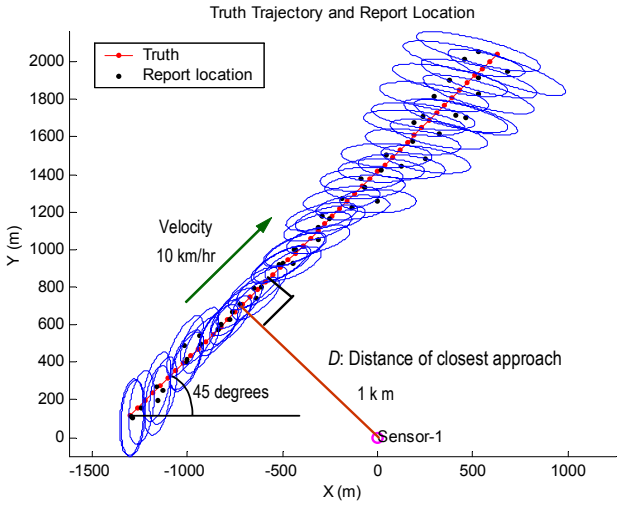

Fig. 1. Target truth trajectory, sensor location, and measurement locations with 0.99 probability error ellipses. The standard deviations for range and azimuth are 20 meters and 3 degrees, respectively.

In order to obtain an initial estimate of the parameter θ, we first perform forward filtering using the extended Kalman filter (EKF) and then perform backward smoothing using the Rauch-Tung-Stribel smoother [2]. We use the Levenberg-Marquardt algorithm [9] in

minimizing the cost function in (2-17) for the ML estimation problem. The true and ML estimated trajectories for the scenario in Fig. 1 are shown in Fig. 2.

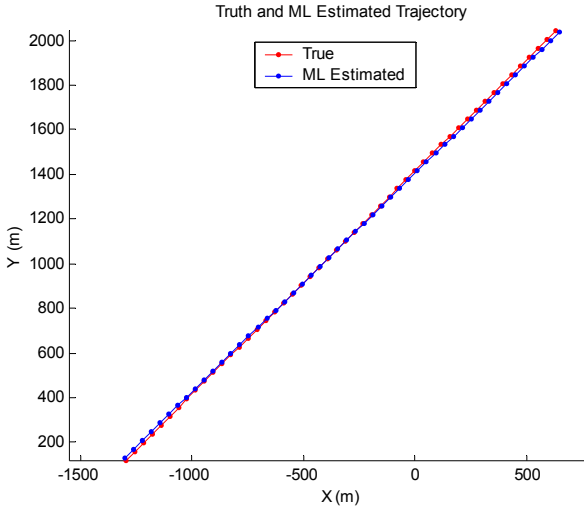

Fig. 2. Target truth trajectory and maximum likelihood estimated trajectory. The distance of closest approach is 1 km. The standard deviations for range and azimuth are 20 meters and 3 degrees, respectively.

We performed 200 Monte Carlo (MC) simulations with different realizations for the measurement error sequence and calculated the parameter-effects curvature and intrinsic curvature. We selected the parameter $\delta := (\theta - \hat{\theta})$ where θ and $\hat{\theta}$ are the true and ML estimated parameters, respectively. We have shown parameter-effects curvatures from 200 MC runs in Fig. 3 and Fig. 4 for scenarios where the distances of closest approach (*D*) are 1 km and 10 km, respectively. The standard deviations for range and azimuth are 20 meters and 3 degrees, respectively. Figures 5 and 6 show the corresponding intrinsic curvatures from 200 MC runs for scenarios where the distances of closest approach (*D*) are 1 km and 10 km, respectively. We observe in Figures 3-6 that the the parameter-effects curvature and intrinsic curvature vary significantly with MC runs for given scenario. Morever, for each scenario, the intrinsic curvature is much smaller compared with the parameter-effects curvature. Figures 3-6, show that both curvature measures increase with increase in the distance of closest approach.

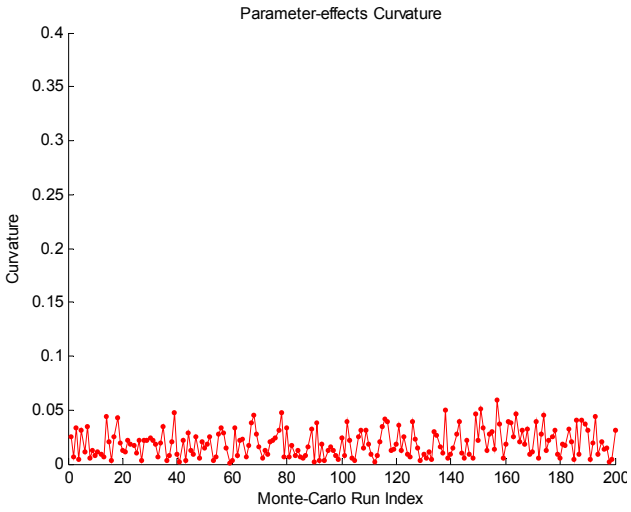

Fig. 3. Parameter-effects curvatures for 200 Monte Carlo runs for the scenario with the distance of closet approach of 1 km. The standard deviations for range and azimuth are 20 meters and 3 degrees, respectively.

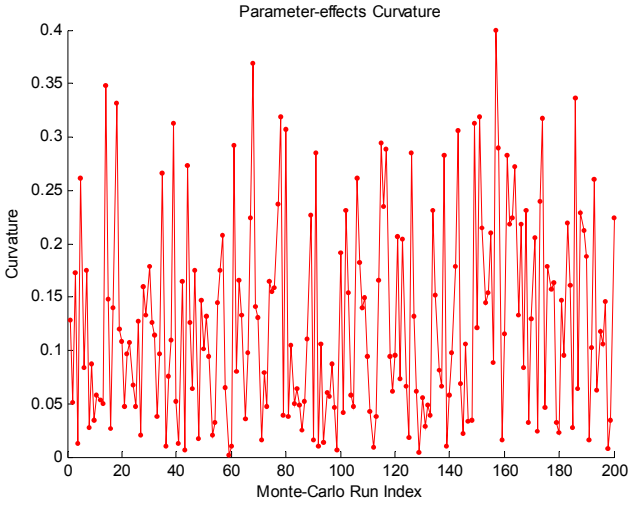

Fig. 4. Parameter-effects curvatures for 200 Monte Carlo runs for the scenario with the distance of closet approach of 10 km. The standard deviations for range and azimuth are 20 meters and 3 degrees, respectively.

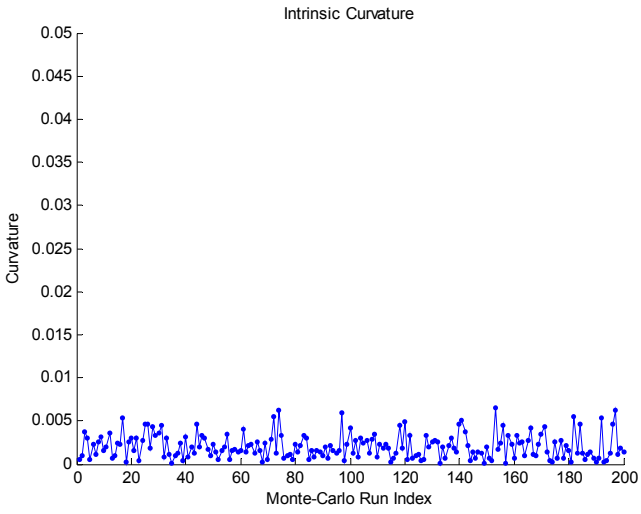

Fig. 5. Intrinsic curvature for 200 Monte Carlo runs for the scenario with the distance of closet approach of 1 km. The standard deviations for range and azimuth are 20 meters and 3 degrees, respectively.

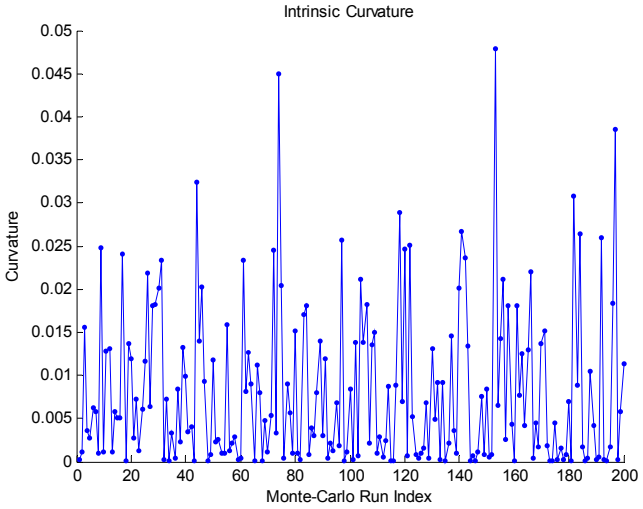

Fig. 6. Intrinsic curvature for 200 Monte Carlo runs for the scenario with the distance of closet approach of 10 km. The standard deviations for range and azimuth are 20 meters and 3 degrees, respectively.

We present the minimum, maximum, median and mean values for the parameter-effects curvature and intrinsic curvature for various values of the distance of closest approach and azimuth measurement error standard deviations in Tables 1 and 2.

Table 1. Parameter-effects curvatures with varying values for the distance of closest approach (*D)* and azimuth standard deviations.

Azimuth Standard Deviation (deg)	*D* (km)	Parameter-effects Curvature			
		min	max	median	mean
3	1	0.0006	0.0587	0.0176	0.0192
	4	0.0004	0.1697	0.0452	0.0524
	10	0.0013	0.3991	0.1062	0.1266
10	1	0.0013	0.5667	0.0967	0.1457
	4	0.0007	1.5763	0.2628	0.3782
	10	0.0017	3.3905	0.4017	0.5639

Table 2. Intrinsic curvature with varying values for the distance of closest approach (*D*) and azimuth standard deviations.

Azimuth Standard Deviation (deg)	*D* (km)	Intrinsic Curvature			
		min	max	median	mean
3	1	0.0001	0.0065	0.0018	0.0020
	4	0.0000	0.0169	0.0020	0.0034
	10	0.0000	0.0478	0.0046	0.0081
10	1	0.0001	0.0065	0.0018	0.0020
	4	0.0000	0.0077	0.0010	0.0015
	10	0.0000	0.0242	0.0029	0.0041

8 Conclusions

In this paper, we have developed an algorithm to quantify the degree of nonlinearity of a nonlinear filtering problem using the *parameter-effects curvature* and *intrinsic curvature* derived from differential geometry. We have presented preliminary results for the constant velocity motion of a target in the XY-plane with two-dimensional range and azimuth measurements. Our results show that the parameter-effects curvature increases with increase in the distance of closest approach of the target from the sensor. For each scenario, the intrinsic curvature is much smaller than the parameter-effects curvature. In our future work, we plan to analyze the performances of the particle filter (PF) [10-12] and EKF with varying degrees of nonlinearity.

References

[1] Y. Bar-Shalom, X. R. Li and T. Kirubarajan, *Estimation with Applications to Tracking and Navigation*, Wiley & Sons, 2001.

[2] A. Gelb, Ed., *Applied Optimal Estimation*, The MIT Press, 1974.

[3] D. M. Bates and D. G. Watts, *Nonlinear Regression Analysis and Its Applications*, John Wiley, 1988.

[4] G. A. Seber and C. J. Wild, *Nonlinear Regression*, John Wiley, 1989.

[5] D. M. Bates and D. G. Watts, "Relative curvature measures of nonlinearity," *J. R. Stat. Soc. B,* Vol. 42, pp. 1-25, 1980.

[6] D. M. Bates, D. C. Hamilton, and D. G. Watts, "Calculation of intrinsic and parameter-effects curvatures for nonlinear regression models," *Commun. Stat.Simul. Comput. B,* Vol. 12, pp. 469-477, 1983.

[7] B. Noble and J. W. Daniel, *Applied Linear Algebra*, Prentice Hall, 1977.

[8] D. Kahaner, C. Moler, and S. Nash, *Numerical Methods and Software*, Prentice Hall, 1989.

[9] J. E. Dennis Jr. and R. B. Schnabel, *Numerical Methods for Unconstrained Optimization and Nonlinear Equations,* SIAM, 1996.

[10] A. Doucet, N. de Freitas, and N. Gordon, Editors, *Sequential Monte Carlo Methods in Practice*, Springer Verlag, 2001.

[11] S. Arulampalam, S. Maskell, N. Gordon, and T. Clapp, "A Tutorial on Particle Filters for On-line Non-linear/Non-Gaussian Bayesian Tracking," *IEEE Transactions on Signal Processing*, Vol. 50, pp. 174-188, 2002.

[12] M. Mallick, T. Kirubarajan, and S. Arulampalam, "Comparison of Nonlinear Filtering Algorithms in Ground Moving Target Indicator (GMTI) Tracking," *Proc. Fourth International Conference on Information Fusion*, August 2001, Montreal, Canada.